Supplementary Information

Real-space Evidence of the Equilibrium Ordered Bicontinuous Double Diamond Structure of Diblock Copolymer

C. Y. Chu,[a] X. Jiang,[b] H. Jinnai,*[b] R. Y. Pei,[a] W. F. Lin,[c] J. C. Tsai[c] and H. L. Chen*[a]

[a]Department of Chemical Engineering and Frontier Research Center on Fundamental and Applied Sciences of Matters, National Tsing Hua University, Hsin-Chu 30013, Taiwan
E-mail: hlchen@che.nthu.edu.tw

[b]Institute for Materials Chemistry and Engineering (IMCE), Kyushu University, 744 Motooka, Nishi-ku, Fukuoka 819-0395, Japan
E-mail: hjinnai@cstf.kyushu-u.ac.jp

[c]Department of Chemical Engineering, National Chung Cheng University, Chia-Yi 62102, Taiwan

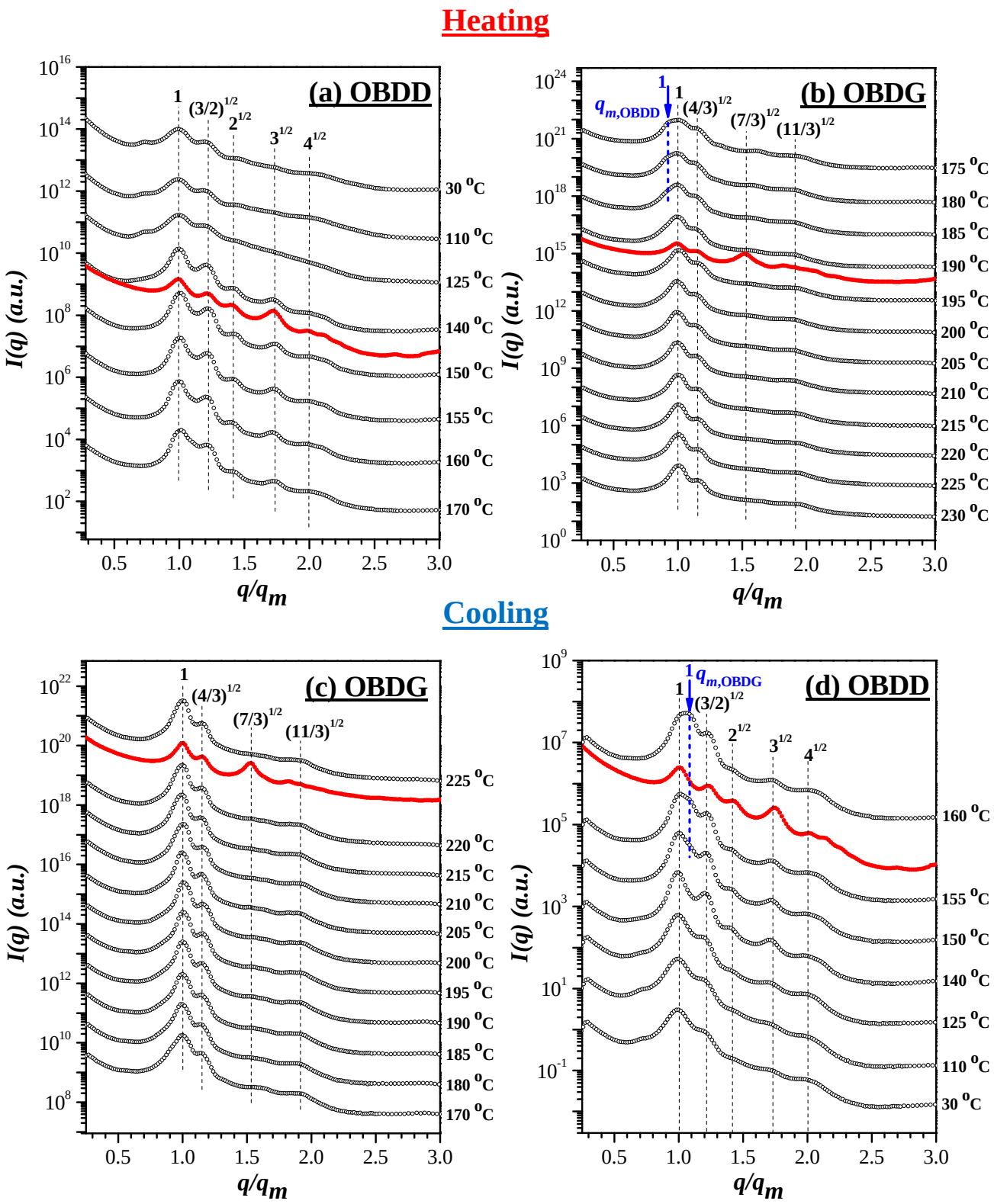

Fig. S1 Temperature-dependent SAXS profiles of the as-cast sPP-*b*-PS films obtained in (a,b) a heating cycle and (c,d) a cooling cycle. The red solid curves shown in (a,d) and (b,c) represent the calculated SAXS curves of the OBDD and OBDG, respectively. The scattering profiles are

presented as a function of q/q_m, with q_m being the position of the primary peak at each temperature. It can be seen that both the OBDD and OBDG structures may coexist at 175 ≤ T (^oC) ≤ 185 in the heating cycle, as the fact of the primary peak of the OBDD is still observed as indicated by blue arrow along with the formation of the OBDG. In the cooling cycle, the coexistence of the OBDD and OBDG structures can be observed again at 160 ≤ T (^oC) ≤ 150.

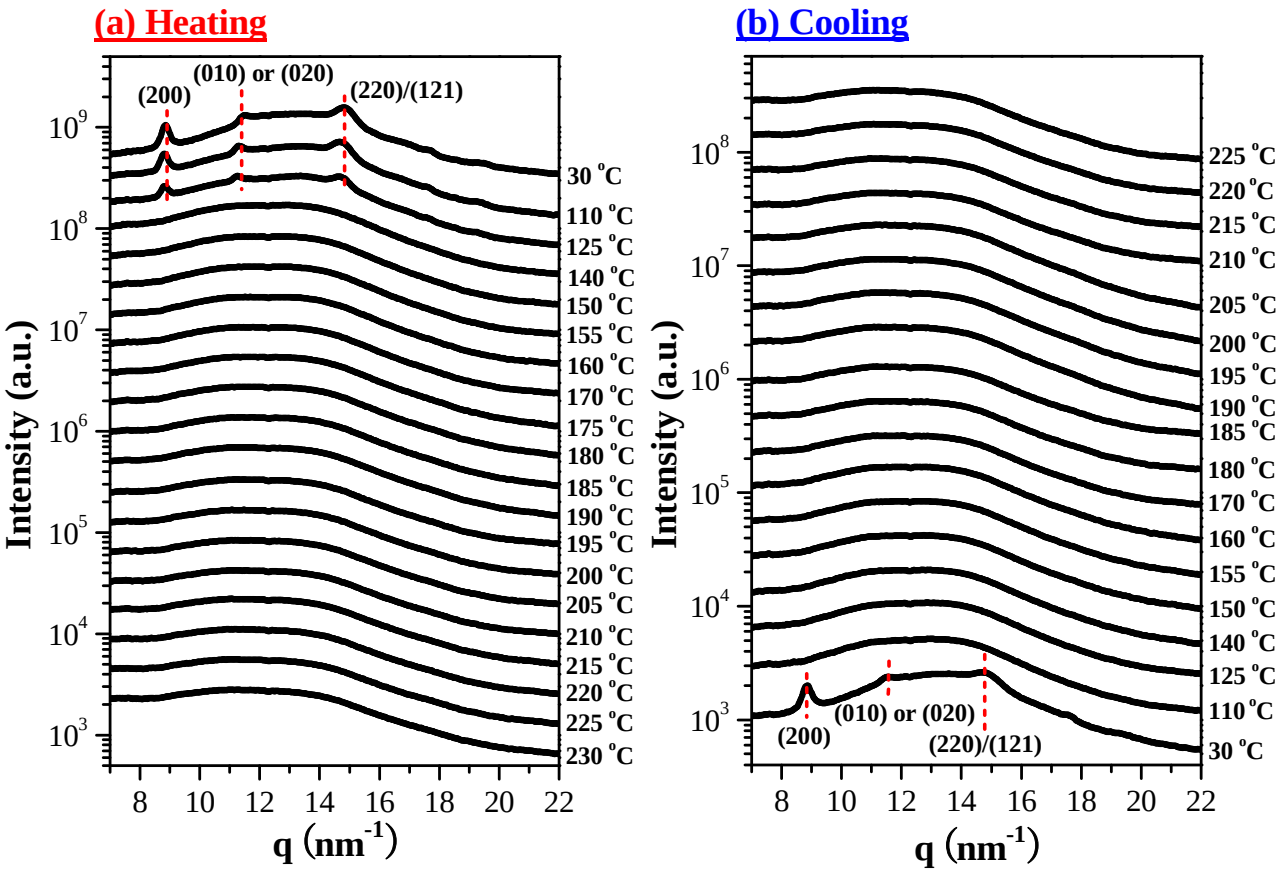

Fig. S2 The corresponding temperature-dependent WAXS profiles of the as-cast sPP-*b*-PS film obtained in (a) a heating cycle and (b) a cooling cycle. The diffraction peaks of sPP crystals vanished above 125 °C, signifying that the crystals have been melted above this temperature.

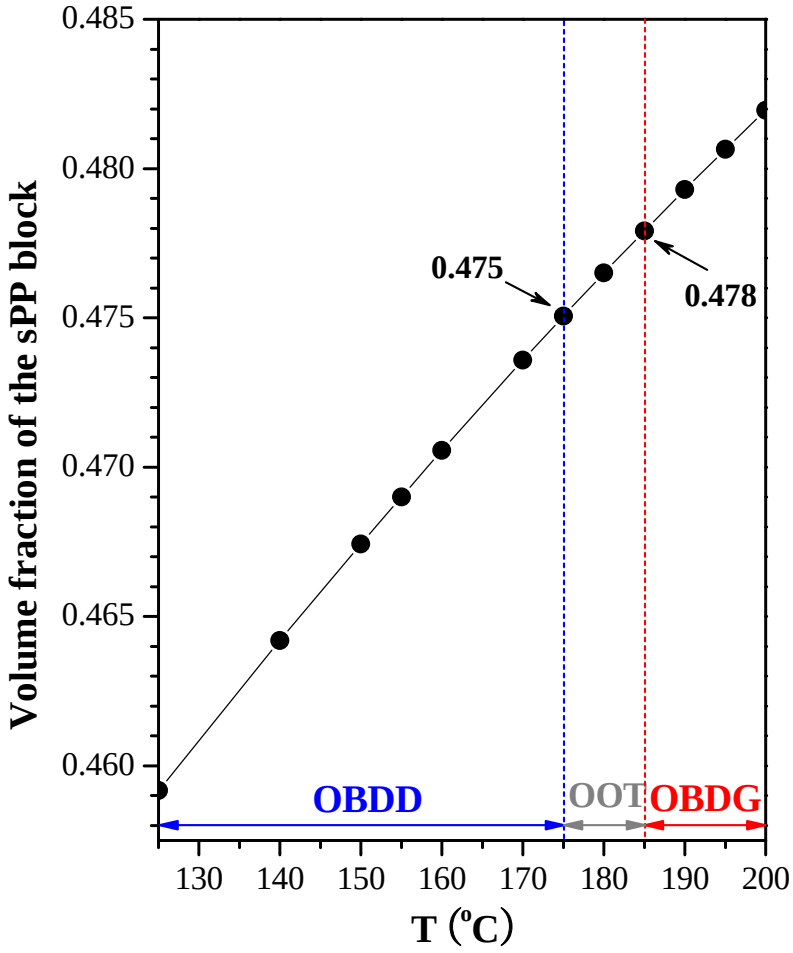

Fig. S3 Volume fraction of the sPP block in the sPP-*b*-PS diblock copolymer as a function of temperature calculated using the densities of sPP and PS reported in the literatures.[47-50] It can be seen that increase of sPP volume fraction was only 0.023 over the temperature range studied. The change, i.e., 0.003, is even smaller across the OBDD-OBDG transition.

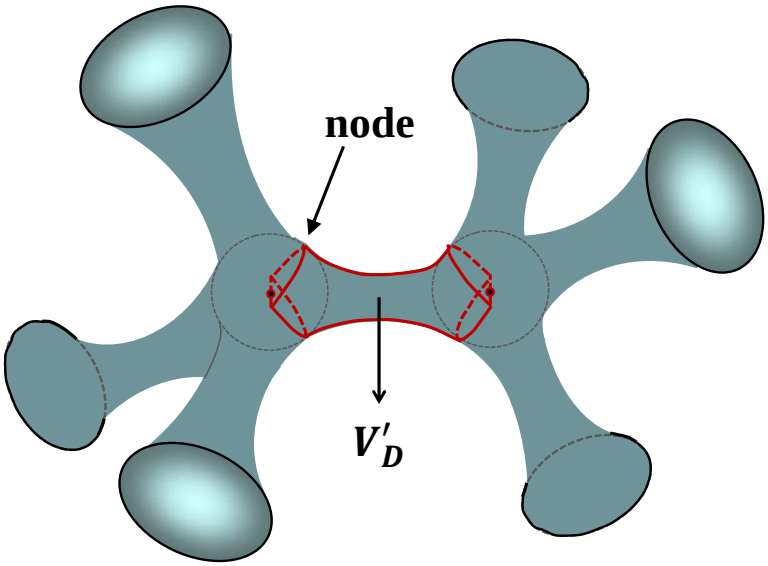

(a) OBDD

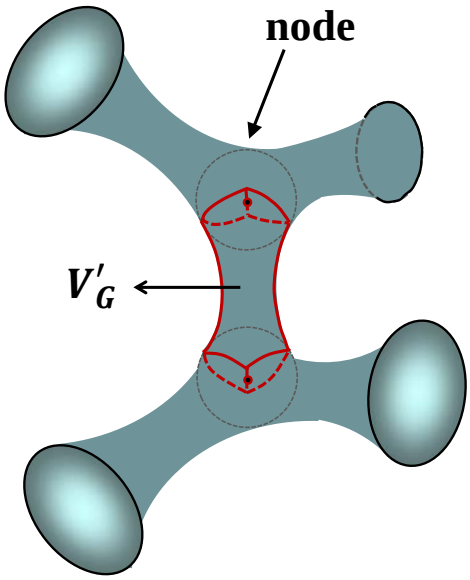

(b) OBDG

Fig. S4 Schematic illustration of the OBDD and OBDG domains.

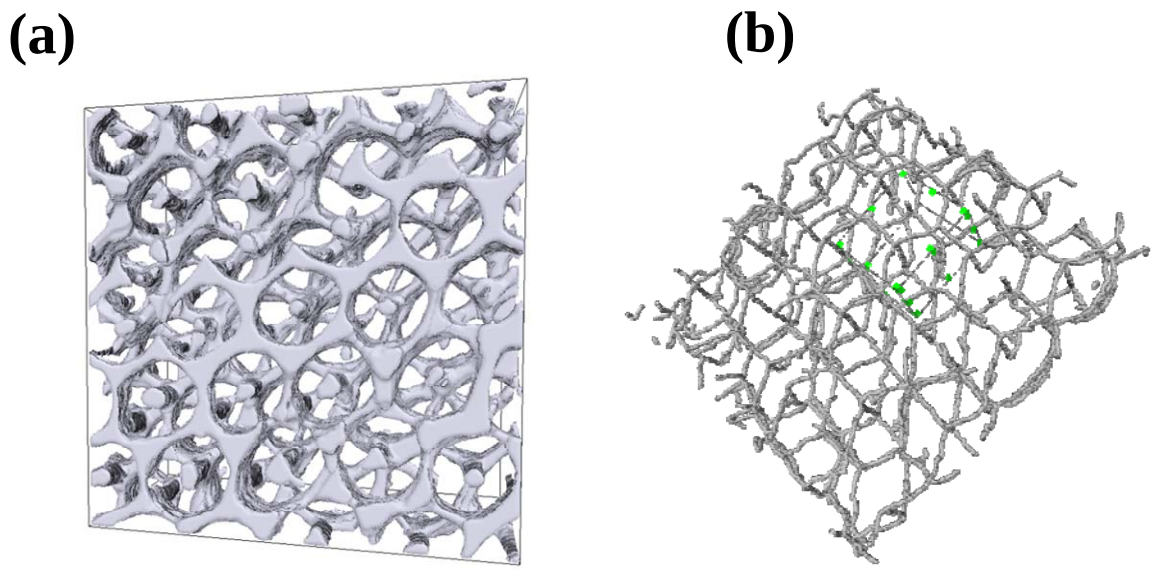

Fig. S5 (a) 3D TEM tomography of the OBDD structure in the sPP-*b*-PS where the microdomains composed of the sPP phase (displayed in gray color) represents the double-diamond lattice with the tetrapod microdomains connected with $Pn\bar{3}m$ symmetry and (6,4) nets. The data shown in (b) reveals the 3D thinned image of the observed OBDD structure.